

AperTO - Archivio Istituzionale Open Access dell'Università di Torino

Phase selection and microstructure refinement of melt-spun Zn_4Sb_3 -type compound

This is the author's manuscript

Original Citation:

Availability:

This version is available <http://hdl.handle.net/2318/149070> since

Publisher:

Springer International Publishing

Terms of use:

Open Access

Anyone can freely access the full text of works made available as "Open Access". Works made available under a Creative Commons license can be used according to the terms and conditions of said license. Use of all other works requires consent of the right holder (author or publisher) if not exempted from copyright protection by the applicable law.

(Article begins on next page)



UNIVERSITÀ DEGLI STUDI DI TORINO

This is an author version of the contribution published on:

Questa è la versione dell'autore dell'opera:

A. Castellero et al., Proceedings of the 11th European Conference on Thermoelectrics:

A. Amaldi and F. Tang (editors), Springer International Publishing, 2014, pagg. 29-35

The definitive version is available at:

La versione definitiva è disponibile alla URL:

http://link.springer.com/chapter/10.1007/978-3-319-07332-3_4

Phase selection and microstructure refinement of melt-spun Zn₄Sb₃-type compound

R. Carlini^{a,b}, A. Castellero^{c,*}, C. Fanciulli^d, F. Passaretti^d, M. Baricco^c, G. Zanicchi^{a,b}

^a *Dipartimento di Chimica e Chimica Industriale - Università di Genova – Via Dodecaneso 31 - 16146 Genova*

^b *INSTM - Unità di Ricerca di Genova - Via Dodecaneso 31, 16146 Genova*

^c *Dipartimento di Chimica e Centro NIS - Università di Torino – via P. Giuria 7 - 10125 Torino*

^d *CNR - Istituto per l'Energetica e le Interfasi - Unità di Lecco - Corso Promessi Sposi 29 – 23900 - Lecco*

** Corresponding autor: Alberto Castellero – email: alberto.castellero@unito.it*

Abstract

The Zn₄Sb₃ phase is considered one of the most interesting compounds for thermoelectric applications in the intermediate temperature range (400-600 K) because of its very low thermal conductivity. Typical processing routes of this material for technological applications require several steps, in order to obtain an homogeneous single phase with fine microstructure.

In this work, melt spinning was used as an intermediate processing step for improving structural homogenization and microstructure refinement of Zn₄Sb₃. The effect of rapid solidification on the phase stability and microstructure was investigated.

Melt spun samples show, on the one hand, other crystalline phases in addition to the expected Zn₄Sb₃-type phase, probably because the high cooling rate did not allow the system to reach the thermodynamic equilibrium. On the other hand, rapid solidification induced a remarkable decrease of crystallites size down to the limit of the nanoscale, as estimated by the peak broadening in the X-ray diffraction patterns and shown by scanning electron micrographs. Additionally, the presence of an irreversible exothermic peak in the DSC trace can be likely related to the crystallization of a small amount of amorphous phase, formed because of the high cooling rate, that could not be detected by XRD.

The results suggest that melt spun flakes can be used as a starting material in the subsequent compaction steps.

Keywords: Zn₄Sb₃; thermoelectric material; rapid solidification, processing.

Introduction

Today an enormous amount of unused waste heat could be converted to electricity by using thermoelectrics solid-state devices[1]. Research in the thermoelectric field covers a lot of different materials such as intermetallics, composites, nanomaterials, etc. [1,2]. Thermoelectric efficiency of these materials can be improved by doping, nanostructuring or non equilibrium syntheses routes [1,3]. Up to now, intermetallics are the most studied materials for thermoelectric applications due to their stability and mechanical properties in thermoelectric devices.

Intermetallic Zn_4Sb_3 compound has raised great interest due to its glass-like thermal conductivity and consequently to its good thermoelectric performance in the intermediate temperature range (400 – 600 K) [2]. Several studies were carried out on this compound to evaluate the influence of different processing routes on its efficiency [4-7]. Processing of this material for technological applications requires several steps, in order to obtain a fully dense homogeneous single phase with fine microstructure [1]. In fact, it is well known that phonon contribution to thermal conductivity can be significantly depressed by a very high density of grain boundaries, leading to an increase of the figure of merit ZT.

Among non equilibrium processing techniques, melt spinning allows fast quenching, promoting the formation of amorphous or metastable phases, together with a significant grain size refinement [8]. Furthermore, the short processing time required strongly reduces contamination due to the working atmosphere. Such a technique could be effective in producing starting materials suitable for further processing, in view of an efficiency increase of thermoelectric properties.

In this paper, the effect of melt spinning on microstructural, structural and thermal properties of Zn_4Sb_3 intermetallic compound is investigated in view of thermoelectric applications.

Experimental

Bulk samples of the intermetallic binary compound Zn_4Sb_3 were synthesized with a simple preparation route. Stoichiometric quantities of zinc and antimony (purity 99.99 mass %) sealed in silica vials under Ar flow were heated up to 750 °C in a muffle furnace, annealed at this temperature for 10 h and, finally, spontaneously cooled.

Rapidly solidified samples of Zn_4Sb_3 were obtained with a melt spinning (MS) apparatus by Edmund Bühler GmbH. The bulk alloy was induction melted in a BN crucible and ejected by an Ar overpressure (0.2 bar) on a copper wheel rotating at 20 m/s.

Chemical analyses of the bulk and melt-spun samples were performed by Induction Coupled Plasma – Atomic Electron Spectroscopy analyses. The ICP-AES system used was an axially-viewed Varian (Springvale, Australia) Vista PRO.

The microstructure and the composition of the samples before and after melting spinning were investigated by scanning electron microscopy and energy dispersive X-ray spectroscopy (EDXS) , using a SEM EVO 40 by Carl Zeiss. Structural characterization was performed by X-ray diffraction (XRD). The measurements were performed on bulk or powdered

samples in the angular range 10° - 100° , with a step of 0.002° , using a PANalytical X'Pert Pro model diffractometer with Cu k_{α} radiation. XRD measurements were also performed using an environmental chamber in order to study the structural evolution of as-spun samples as a function of temperature. Refinement of the XRD pattern was performed using Rietveld method by Full Prof Suite software in order to determine the lattice parameters and the relative phase fractions.

Thermal stability of the samples was investigated by differential scanning calorimetry (DSC) using a power compensation Perkin Elmer Diamond DSC.

Results and discussion

X-ray diffraction analyses of the bulk samples show only the reflections of the ϵ - Zn_4Sb_3 equilibrium phase (not shown here), in accordance with the chemical composition measured by ICP ($\text{Zn}_{57.3}\text{Sb}_{42.7}$ at.%) and the equilibrium phase diagram [9]. The first DSC heating cycle of the bulk sample, Figure 1(a), shows a sequence of four endothermic signals between 409°C and 411°C , around 440°C , 493°C and 532°C . The sequence of endothermic peaks can be explained by the invariant reactions proposed in the equilibrium phase diagram. However, the two signals at lower temperature ($409 - 411^{\circ}\text{C}$ and 440°C) are not compatible with the nominal and measured composition, suggesting that the sample is not fully homogeneous, and can be related to the presence of a small amount of regions richer in Zn due to local fluctuation of the chemical composition. In the second DSC heating cycle, the first two peaks disappear, while those at higher temperature are reproduced, indicating that after the first DSC heating cycle the sample results chemically homogeneous.

The XRD pattern of the as-spun sample (pattern at 30°C start, in Figure 2) shows the presence of the equilibrium phase ϵ - Zn_4Sb_3 and additional phases that could not be indexed. On the basis of the phase diagram, it is likely that some high temperature phase has been retained as a consequence of the rapid quenching. The broadening of the reflections suggests that a highly defective microstructure was produced by rapid solidification. Furthermore, the low intensity of the pattern and the relative high value of baseline at low angle reflections, suggests the presence of amorphous phases consistent with the rapid solidification proper of the melt spinning process. The values obtained for the lattice parameters of the rhombohedral cell (R, $-3c$) are in agreement ($a = 1.2228\text{ nm}$, $c = 1.2424\text{ nm}$) with those reported in the literature for the ϵ - Zn_4Sb_3 phase [10,11].

The microstructure of the as spun sample is shown by the SEM micrographs in Figure 3. The as spun sample reveal a cross section about $2\text{-}10\text{ }\mu\text{m}$ thick, Figure 3(a), and a fine microstructure constituted by small elongated particles (about $2\text{ }\mu\text{m} \times 6\text{ }\mu\text{m}$), Figure 3(b), which are separated by small pores.

The DSC measurements of the as spun sample, Figure 1(b), show as main feature a sequence of two irreversible exothermic signals between 200 °C and 260°C that disappear in the second heating cycle. Such signals are compatible with the presence of amorphous or other metastable phases that irreversibly transform to more stable phases.

The structural evolution of the spun samples as a function of temperature is shown in Figure 2. The XRD pattern at 200 °C does not show any significant variation with respect the one measured at 30 °C (start). At 285 °C the pattern clearly shows the disappearance of the peaks related to secondary metastable phases and the appearance of some peak related to the phase ZnSb (oP16-CdSb) as indicated by the star in Fig. 2. Furthermore, the signal/baseline ratio tends to become higher after annealing at 285 °C and the profile of the crystallographic reflections becomes sharper indicating the occurrence of a recrystallization process and the disappearance of an amorphous phase responsible for the low intensities observed in the pattern of the as spun sample. Finally, the XRD pattern at 30 °C (end) after the thermal cycle confirms the presence of the same phases formed at 285 °C indicating that the structural transformation into the equilibrium phases ZnSb and ϵ -Zn₄Sb₃ is irreversible and compatible with the transformation observed by DSC.

On the basis of the results obtained, it can be concluded that rapid solidification is a suitable technique for producing in a controlled way (i.e. no contamination, short processing time) microstructurally refined ϵ -Zn₄Sb₃, that can be successfully used in the subsequent compaction step [12].

Conclusions

Melt spinning was used as an intermediate technique in the processing sequence for the preparation of thermoelectric Zn₄Sb₃.

Rapid solidification leads to a non equilibrium solidification path with the possible formation of amorphous and metastable phases, together with the desired ϵ -Zn₄Sb₃ equilibrium phase. The broadening of the XRD patterns indicates the presence of a highly defective microstructure. From the morphological point of view, the as spun samples are characterized by thin foils (2 - 10 µm) constituted by an agglomeration of small elongated particles (around 2 µm wide and 6 µm long).

Irreversible transformations of the metastable phases in the as spun sample was evidenced by DSC measurements and X-ray diffraction analysis upon heating, showing the formation of the ZnSb and ϵ -Zn₄Sb₃ equilibrium phases after thermal cycling up to 285 °C.

Acknowledgements

The authors would like to thank Dr. Gianluca Fiore for the support in the preparation of the rapidly solidified samples by melt spinning, Dr. Francesco Soggia for the ICP-AES analyses and Dr. Elena Villa and Enrico Bassani for their support in ODP processing and mechanical characterizations.

References

- [1] D. M. Rowe, Thermoelectrics handbook—Macro to Nano, (CRC Press Inc., Florida 2005)
- [2] G. J. Snyder, E. S. Toberer, Nat. Mater. 7, 114 105-114 (2008)
- [3] G. S. Nolas, J. Sharp, H. J. Goldsmid, Thermoelectrics—Basic Principles and Materials Development, (Springer Series in Materials Science, Springer, Berlin, 2001), vol. 45
- [4] L. Pan, X. Y. Qin, M. Liu, F. Liu, J. Alloys Compd. 489, 228 228-232 (2010)
- [5] E. S. Toberer, P. Rauwel, S. Gariel, J. Taftø, G. J. Snyder, J. Mater. Chem., 20, 9877–9885 (2010)
- [6] F. Liu, X. Y. Qin, H. X. Xin, J. Phys. D 40, 24 7811-7816 (2007)
- [7] C. Stiewe, T. Dasgupta, L. Bottcher, B. Pedersen, E. Muller, B. Iversen, J. Electr. Mat. 39, 9 1976-198 (2010)
- [8] M. Baricco, E. Bosco, E. Olivetti, M. Palumbo, P. Rizzi, A. Stantero, L. Battezzati, Int. J. Mater. Prod. Tec. 20, 358 (2004)
- [9] Okamoto H. Phase diagram binary alloys (Materials Park, OH, USA 2000)
- [10] R. Carlini, D. Marré, I. Pallecchi, R. Ricciardi, G. Zanicchi, Intermet. 45, 60-64 (2014)
- [11] Y. A. Mozharivskyj, A. O. Pecharsky, S. L. Bud'ko, G. J. Miller, Chem. Mater. 16, 1580-1589 (2004)
- [12] C. Fanciulli, R. Carlini, A. Castellero, F. Passaretti, M. Baricco, G. Zanicchi, submitted to the 11th European Conference on Thermoelectrics, 18-20 November 2013, Nordwijk, The Netherlands.

Figures captions

Fig. 1. DSC traces of the bulk sample at 2 °C/min, (a), and the as spun sample at 20 °C/min, (b).

Fig. 2. X-ray diffraction pattern of the as spun ribbon as a function of temperature: 30 °C (start), 200 °C, 285 °C and 30 °C (end).

Fig. 3(a). Secondary electron SEM micrograph showing the cross section of the as spun sample.

Fig. 3(b). SEM micrograph showing the texture of the as spun sample, constituted by small elongated particles divided by submicrometric pores. Left image: secondary electron detector. Right image: backscattered electron detector.

Figure 1

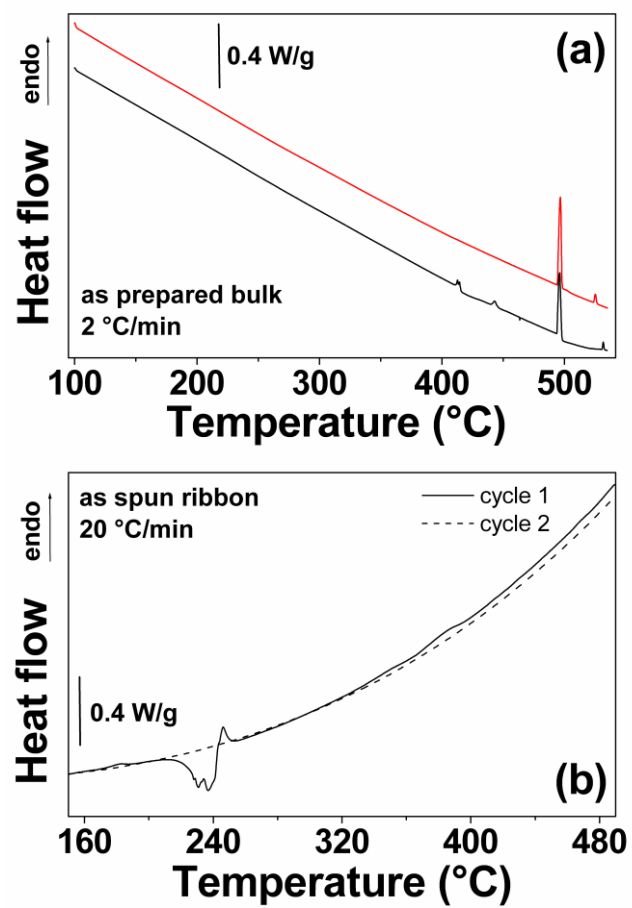


Figure 2

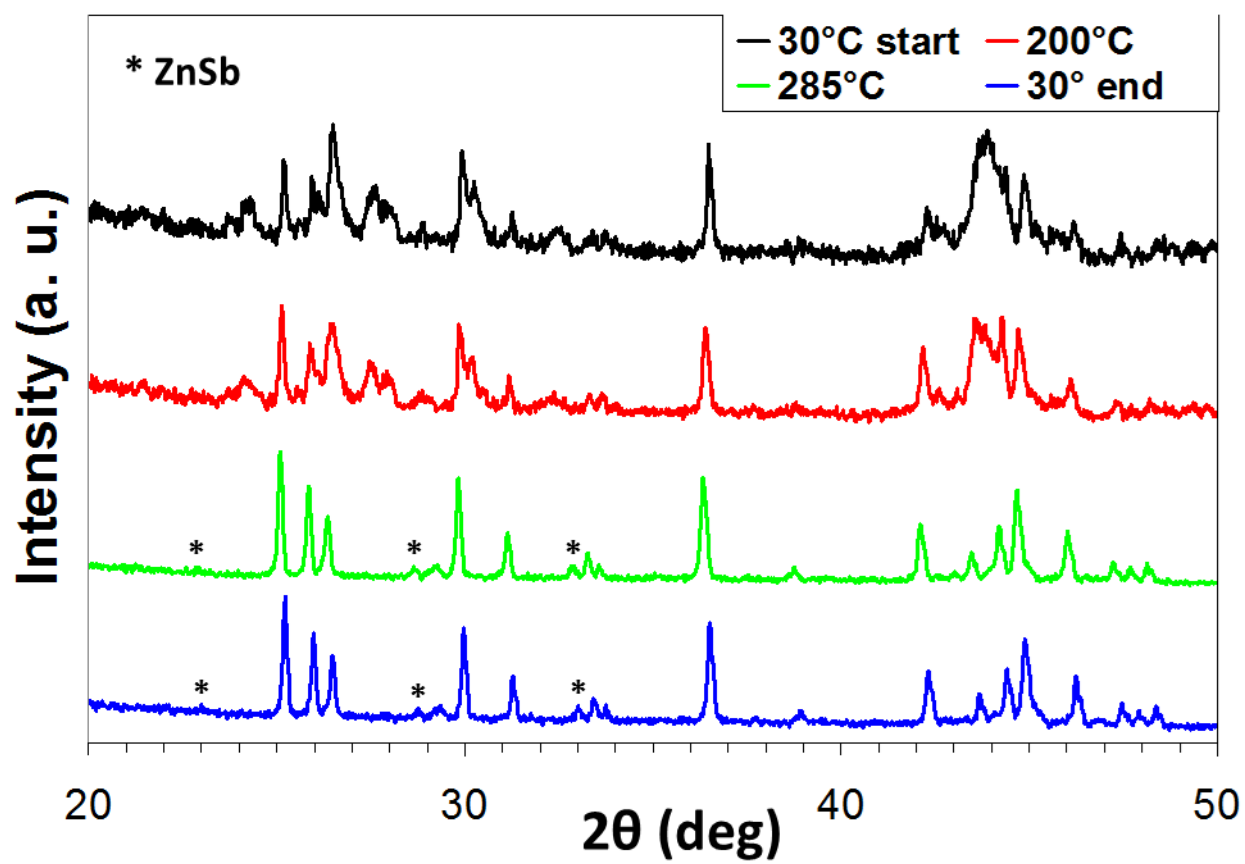


Figure 3(a)

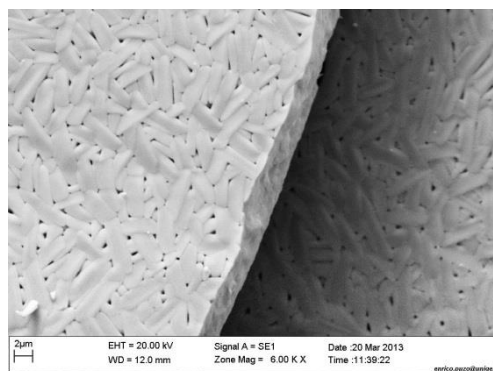


Figure 3(b)

